We are IntechOpen, the world's leading publisher of Open Access books Built by scientists, for scientists

4,800
Open access books available

122,000
International authors and editors

135M
Downloads

Our authors are among the

154
Countries delivered to

TOP 1%
most cited scientists

12.2%
Contributors from top 500 universities

CLARIVATE ANALYTICS BOOK CITATION INDEX INDEXED

WEB OF SCIENCE™

Selection of our books indexed in the Book Citation Index in Web of Science™ Core Collection (BKCI)

Interested in publishing with us?
Contact book.department@intechopen.com

Numbers displayed above are based on latest data collected.
For more information visit www.intechopen.com

27

Modulation of Multidrug Resistance on the Same Single Cancer Cell in a Microfluidic Chip: Intended for Cancer Stem Cell Research

XiuJun Li,[1,2] Yuchun Chen[2] and Paul C.H. Li[2]
[1]*Harvard University, Department of Chemistry and Chemical Biology*
[2]*Simon Fraser University, Department of Chemistry*
[1]*USA*
[2]*Canada*

1. Introduction

A small population of cancer stem cells has been identified in a range of haematopoietic and solid tumours. These cells retain features of normal stem cells including self-renewal, pluripotency and altered gene expression, and might represent the cell of origin of these tumours (Dean et al., 2005)(Fallica et al., 2011). The possible eradication of cancer stem cells might offer revolutionary advances in the treatment of cancer. However, cancer stem cells are rare and are hard to destroy due to the occurrence of high level of multidrug resistance (MDR) proteins.

Tumor cells carrying the MDR phenotype are often associated with the over-expression of drug efflux pumps, among which the membrane-bound energy-dependent P-glycoprotein (Pgp) is one of the important classes (Marthinet et al., 2000)(Persidis, 1999)(Locke et al., 2003). The Pgp efflux pump, which belongs to the superfamily of ATP binding cassette (ABC) transporters (i.e. ABCB1) (Higgins, 2007) and is encoded by the MDR1 class of genes (Gros et al., 1986), actively transports drugs out of the cancer cells. This has caused the intracellular drug concentration to be lower than the drug's efficacy threshold within cancer cells (Marthinet et al., 2000), leading to the failure of many forms of chemotherapy (Higgins, 2007). Gaining a better insight into the mechanisms of cancer stem cell resistance to chemotherapy might lead to new therapeutic drug targets and better anti-cancer treatment strategies (Dean et al., 2005)(Shervington and Lu, 2008)(Dean, 2009)(Donnenberg and Donnenberg, 2005).

To improve the chemotherapy sensitivity, Pgp inhibitors or MDR modulators have been employed, with their effects on MDR reversal studied (Ren and Wei, 2004)(Wang et al., 2000)(Efferth et al., 2002)(Medeiros et al., 2007)(Meaden et al., 2002). For instance, Ren *et al.* studied the efflux of doxorubicin in human carcinoma cells (Ren and Wei, 2004). But the assay conducted by a fluorescence plate reader is not amendable to the study of rare cells such as cancer stem cells. Wang *et al.* developed a method to quantitatively assess Pgp inhibitors by flow cytometry (Wang et al., 2000). While this method is widely used to study MDR modulation, it does not provide the information of an individual single cell, such as its time-dependent drug transport kinetics. In addition, flow cytometry requires a large

number (i.e. 100,000) of cells in the starting population to achieve reliable results (Wang et al., 2005). This is a challenging requirement especially when only a limited amount of rare cells is available.

Since 2000, the microfluidic technique has been widely used for cell biology applications (Li and Li, 2010)(Salieb-Beugelaar et al., 2010). This technique has several advantages for conducting cellular assays: (1) the liquid channels or physical microstructures are compatible with the micrometer-sized biological cells, and these features make single-cell manipulation, or single-cell capture most applicable; (2) the microfluidic devices can be used to analyze a small amount of cells, and this aspect is advantageous in bioanalytical applications because biological samples are often limited in quantity; (3) this technique has a low reagent consumption, and this reduces the assay costs; and (4) the microfluidic technique can integrate multiple steps on a single microdevice, including cell sample introduction, fluid control, single-cell capture, cell lysis, reagent mixing, and analyte detection.

In cellular applications, single-cell analysis is preferred to the traditional bulk cellular analysis because the former can study cellular heterogeneity and provide information on cell-to-cell variations (Sims and Allbritton, 2007)(Li and Li, 2010)(Di Carlo and Lee, 2006). Additionally, physicochemical modelling of biological processes also demands data to be obtained from a single cell (El-Ali et al., 2006). To date, the single-cell applications using the microfluidic devices include intracellular signalling (Li and Li, 2005)(Wheeler et al., 2003)(Li et al., 2004), pathogen identification(Zeng et al., 2010), myocyte contraction (Li and Li, 2005)(Li et al., 2007)(Cheng et al., 2006)(Klauke et al., 2003), drug discovery (Li et al., 2009)(Li et al., 2007), patch-clamp recording (Chen and Folch, 2006), multidrug resistance (Li et al., 2008), cell nanosurgery(Jeffries et al., 2007), electroporation (Ryttsen et al., 2000), genetic analysis (Liu et al., 2010)(Hong et al., 2004), protein analysis (Schumann et al., 2008), forensic analysis (Liu et al., 2010), cell culture (Peng and Li, 2004), photobleaching of cellular fluorescence (Peng and Li, 2005), and so on.

Recently, we have developed a microfluidic single-cell analysis approach for the study of multidrug resistance modulation by real-time monitoring of drug efflux in MDR cancer cells (Li et al., 2008). In order to distinguish drug effects of MDR modulators on cancer cells, control experiments on untreated cells are needed, but cell heterogeneity in multidrug resistance can obscure any positive drug response. To address this issue, we have introduced and tested the concept of same-single-cell analysis (SASCA) in which the same cell is used as its control in order to compare the effect of MDR modulators on drug efflux (Li et al., 2008). In addition to measuring drug efflux, we have also developed a new microfluidic approach to study MDR modulation effects of drug candidates by monitoring drug accumulation.

2. Methodology

This section will briefly introduce the design of the microfluidic chip, followed by the procedures for single-cell selection and retention, and the same-single-cell approaches for drug efflux and drug accumulation measurements. Finally, the procedures for conventional cell assays such as flow cytometry and cytotoxicity tests are listed.

2.1 Microdevice design and fabrication

The layout of the glass microfluidic chip is shown in Figure 1a. The chip consists of 3 channels, 3 reservoirs and 1 chamber containing a cell retention structure. Reservoir 1 is

used to introduce cells; reservoir 2 serves as the waste outlet, and reservoir 3 is used for reagent delivery. The glass chip was fabricated by Canadian Microelectronic Corporation (CMC, Protolyne® Chip) by the standard microfabrication procedure, with a channel depth of 20 μm (Manz et al., 1992). An image of the microchip filled with a red food dye is shown in Figure 1b. Figure 1c illustrates the 3-dimensional view of the cell retention structure, with the retained single cell treated with a flow of drug solution.

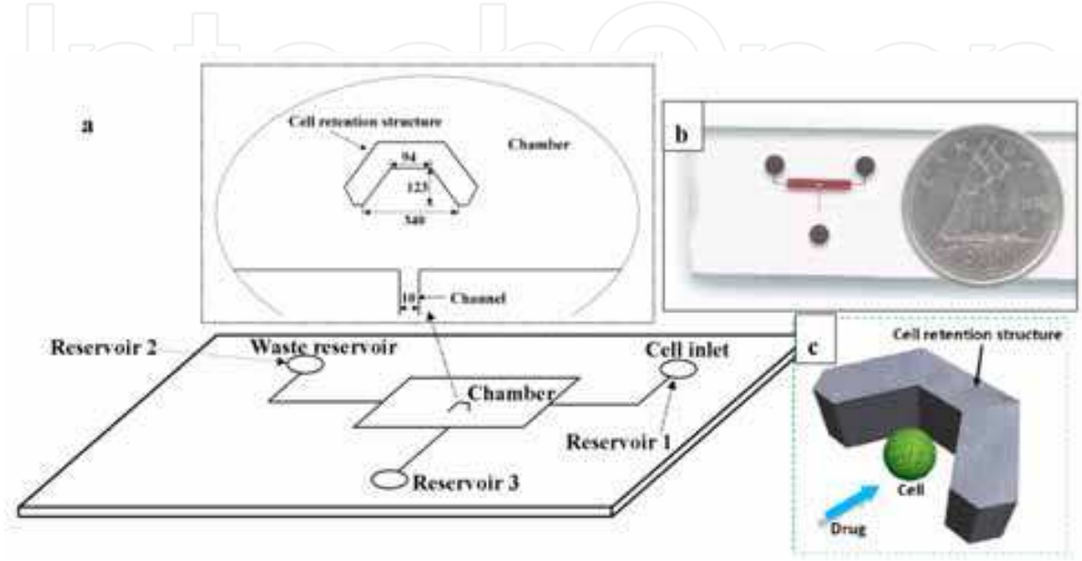

Fig. 1. Layout of the microfluidic chip. (a) The schematics of the microfluidic chip consisting of 3 solution reservoirs and a cell retention structure, with the dimensions (in μm) shown in the inset. (b) An image of the microchip filled with a red food dye. A Canadian dime (10-cent coin) was placed on the chip for size comparison. (c) A schematic diagram of the 3-dimensional illustration of the cell retention structure. Reprinted with permission from American Chemical Society and Royal Society of Chemistry (Li et al., 2008; Li et al., 2011)

2.2 Cell culture

The human wild-type (WT) T-cell leukemic cell line CCRF-CEM (CEM/WT, drug-sensitive) was obtained from ATCC. This cell line and its multidrug-resistant vinblastine-selected subline (CEM/VLB0.05, drug resistant) were maintained in α-MEM medium supplemented with 10% fetal bovine serum and 50 U/mL penicillin, as previously reported (Li et al., 2008).

2.3 Single-cell selection and retention

After a cell suspension (~0.1 x 10^6 cells/mL) was introduced into reservoir 1, the cells flowed unidirectionally (from the right to the left) into the microchip. By adjusting the liquid levels of reservoirs 1 and 2, a desired cell was adjusted to flow near the entrance of the cell retention structure. Then, a liquid flow at the central reagent channel was induced to direct the cell into the retention structure. The cell was allowed to settle further for ~ 15 min (900 s) before the fluorescence measurement was started. Figure 2 shows the image of a single CEM/VLB cell retained in the cell retention structure. The post-retained cell remained alive, which was confirmed using a live stain (i.e. fluorescein diacetate), as shown in the inset of Figure 2. This approach has been widely used to selectively retain single round-shaped

cancer cells and rod-shaped cardiomocytes (Li and Li, 2005; Li and Li, 2006; Li et al., 2007; Li et al., 2008; Li et al., 2009; Li et al., 2011)

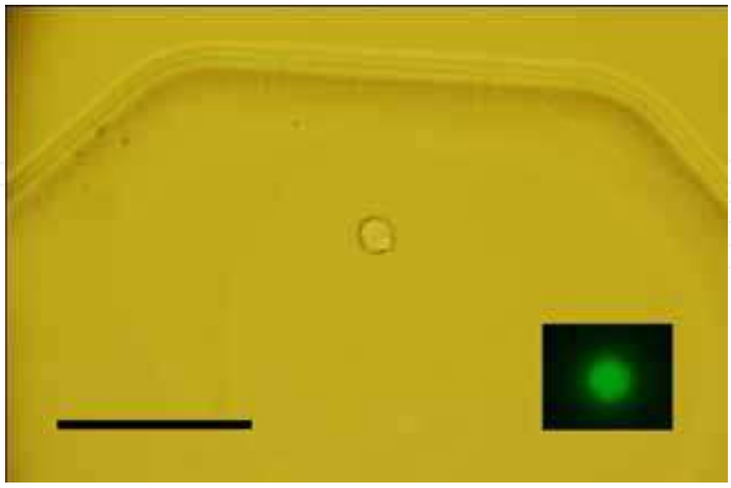

Fig. 2. An optical image of a retained live single CEM/VLB cell, which had been stained by fluorescein diacetate (25 μM) as shown in the inset. The scale bar is 50 μm. Reprinted with permission from American Chemical Society (Li et al., 2008)

2.4 On-chip drug efflux study on single cells

As previously described, an optical detection system was employed for simultaneous bright-field observation and fluorescence measurement (Li et al., 2009). We measured the uptake of the drug daunorubicin (DNR) because it is a substrate of the MDR1 transporter (Murthy and Shah, 2007) (Fu and Roufogalis, 2007), and we used the fluorescent method since DNR is inherently fluorescent (i.e., λ_{em}=590 nm, λ_{ex}=470 nm). The chip was shuttled back and forth across the detection aperture window so that the signals for the cell or its vacant region in the cell medium were obtained in turn. When the cell was inside the detection aperture, the cellular fluorescence was measured; whereas the background signal was measured when the cell was outside the detection window.

We have conducted experiments using two methods: different-single-cell analysis (DISCA) and same-single-cell analysis (SASCA). In the DISCA method, after one CEM cell was selected and retained in the cell retention structure, the cell media in all the reservoirs were removed, and then reservoir 3 was filled with DNR (35 μM) and left to flow in the microchannel for ~1000 s. There was virtually instantaneous replacement of the cell medium around the cell by the DNR solution because the space in front of the cell retention structure was small. Fluorescent measurement was initiated to observe DNR accumulation in the cell (e.g. Cell 1), see Figure 3a. After the accumulation stage, the solutions in all reservoirs were replaced by the cell medium (i.e. no DNR) and it was left to flow for ~1800 s. At the same time, the cellular fluorescent intensity during drug efflux in the cell medium was measured.

This procedure was repeated on a second retained cell (e.g. Cell 2). Briefly, it was treated with 35 μM DNR for ~1000 s, and drug efflux was conducted in cell medium containing a MDR inhibitor candidate compound (i.e. VER, IQ or ART) for ~1800 s. The two sets of fluorescent intensity curves are depicted in the schematics shown in Figure 3a. Comparison of the 2 drug efflux curves (Ed1 vs Ed2) were made subsequently, see Figure 3a inset.

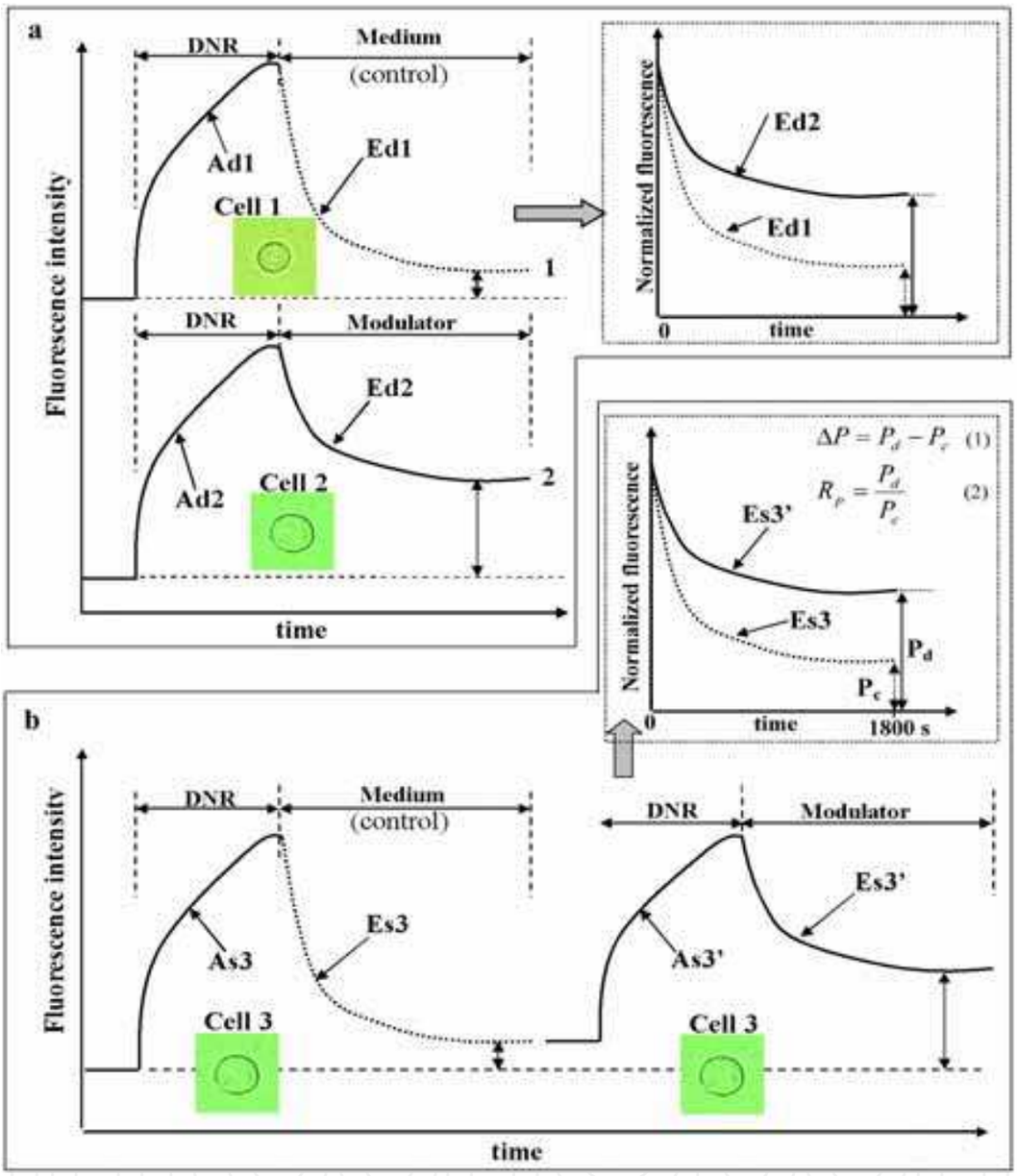

Fig. 3. The schematic illustration of DISCA and SASCA for single-cell MDR efflux study. (a) In DISCA, two different cycles of accumulation and efflux occur on two different cells, namely cell 1 (Ad1 and Ed1), and cell 2 (Ad2 and Ed2). MDR modulation is evaluated by comparing the normalized fluorescent intensity of Ed2 and that of Ed1 (different cell control) shown in the inset. (b) In SASCA, one and the same cell was used in the 2 cycles of drug accumulation (As3, As3') and efflux (Es3, Es3'). MDR modulation is evaluated by comparing the normalized fluorescent intensity of Es3' with that of Es3 (same cell control) shown in the inset. P_d and P_c are the DNR retention percentages in the MDR modulator solution, and in the medium alone (control) at efflux time of 1800 s, respectively. These percentages are determined by dividing the cell fluorescent intensity at efflux time of 1800 s, with the maximum fluorescent intensity before the efflux stage. Reprinted with permission from American Chemical Society (Li et al., 2008)

In the same-single-cell analysis (SASCA) method, only one retained cell (e.g. Cell 3) was used. It was first treated with 35 μM DNR for ~1000 s in the drug accumulation stage. Thereafter, drug efflux was observed in cell medium alone for ~1800 s (control experiment). Then, the same cell was treated a second time with 35 μM DNR for ~1000 s, and a second drug efflux was observed in cell medium containing a MDR inhibitor candidate compound (i.e. VER, IQ or ART) for ~1800 s. The fluorescent intensity curves are depicted in the schematics shown in Figure 3b. Comparison of the 2 efflux curves (Es3 vs Es3′) are shown in Figure 3b inset. The time needed to complete this procedure was ~115 min, as described in our previous report (Li et al., 2008).
After all drug treatments and cell measurements, trypan blue was used to treat the cell in order to evaluate the cell viability.

2.5 On-chip drug accumulation study on single cells

In SASCA, only one retained cell (e.g., cell 3) was used. The cell was first treated with DNR (8.8 μM) in the absence of MDR modulators for ~1400s to test drug accumulation (control experiment). Thereafter, the same cell was treated with a DNR solution in the presence of a MDR modulator for ~700 s. Since we expect that if the modulator has a positive drug effect, there is greater drug accumulation, as displayed by the instant change of the slope depicted in Figure 9b.

2.6 Flow cytometry

Flow cytometry was performed using a fluorescence-activated cell sorter (FACS) to confirm the microfluidic single-cell analysis results, utilizing a previously reported procedure (Wang et al., 2000). Briefly, an aliquot (750 μL) of the cells (300,000 cells/mL) in the cell culture medium was transferred to a plastic tube containing 750 μL of incubation medium with DNR (35 μM). Drug accumulation was conducted at 23 °C for 30 min in the dark. After centrifugation (200 g for 5 min) and removal of the supernatant, the cells were re-suspended in the cell medium alone (i.e. without DNR) and incubated at 23 °C for an additional 30 min (the efflux phase). After removing supernatant, cold HBSS was then added to each tube to quench the drug efflux. The cell suspension was transferred to a FACS tube, and was stored on ice (for less than 15 min) before analysis. Fluorescent intensity (excitation at 488 nm, emission at 570 nm) was measured and displayed as single-parameter histograms, based on the acquisition of data from 10,000 cells. The procedure was repeated for the efflux study of the cells in the presence of a MDR modulator compound (e.g. VER, IQ and ART). The time needed to complete this procedure was ~149 min. as described previously (Li et al., 2008).

2.7 MTT cytotoxicity assay

The sensitivities of CEM/WT cells and CEM/VLB cells to the cytotoxic drug DNR were determined by the 96-well microtiter plate assay (Jow et al., 2004; Li et al., 2009). To summarize, after 1 day of cell seeding in each well, 100 μL of test compounds at various concentrations were separately introduced in each well. After the cells were further incubated for 3 days, 40 μL of MTT (5 mg/mL) was added to each well and incubated at 37 °C for 3 h. Finally, after removing the supernatant and adding DMSO, a microplate reader was used to measure the absorbance of each well at 570 nm. The medium without test compounds and DMSO alone were used as the negative control and the positive control, respectively. All tests were carried out in triplicate.

3. Results and discussion

3.1 Multidrug resistance and drug sensitivity

We first investigated the different drug responses of the drug-resistant cells (i.e. VLB cells) and the wild-type (WT) cells using the MTT cytotoxicity assay. Since VLB cells, but not WT cells, have over-expressed Pgp pumps, this discrepancy leads to the difference in the drug sensitivities of these two types of CEM cells toward the drug DNR. This difference was confirmed by the results of cytotoxicity assay (see Figure 4a). It is estimated that the IC_{50} values of DNR (half maximal inhibitory concentration of a drug) for CEM/WT and CEM/VLB0.05 are ~80 nM and 15 μM, respectively. Thus, the CEM/VLB cells are ~180 fold more resistant to DNR, as compared to the CEM/WT cells. This higher drug resistance of the MDR cancer cells is a primary cause of chemotherapy failure, when patients develop multidrug resistance.

3.2 Different-single-cell analysis (DISCA) for drug efflux study in a microchip

The purpose of this drug efflux study was to test a MDR modulator compound (e.g. verapamil or VER) for a possible MDR reversal effect. To achieve this, DNR efflux was conducted on a CEM/VLB cell (test cell) in the presence of the modulator compound and then on another cell (control cell) in the absence of the compound. Since two cells are measured, this analysis is called different-single-cell analysis (DISCA). As described in Figure 3a inset, the two efflux curves (Ed1 vs Ed2) obtained from the two different cells (i.e. Cell 1 and Cell 2) were compared.

In the results shown in Figure 5a, we observe the typical drug efflux curves of different single drug-resistant cells (CEM/VLB) in various DNR-free solutions such as VER, IQ, and the cell medium alone. It was observed that the DNR efflux was initially fast (i.e. 0-500 s). Afterwards, the efflux rate slowed down and the cellular fluorescence did not change significantly. In addition, less DNR was retained (i.e. 0.2-0.4 or 20-40%) when the efflux was conducted in the medium (the efflux-in-medium curve) as compared to the efflux conducted in VER (the efflux-in-VER curve). This observation is consistent with the notion that VER interferes with the drug efflux process by binding to the Pgp efflux pump, thus resulting in more DNR retention (Akiyama et al., 1988; Wang et al., 2000). We also studied the MDR effect of another compound, IQ, an ingredient of the traditional Chinese herb licorice (Sung and Li, 2004; Cai and Li, 2007). It has been reported that IQ has an anti-tumor effect on human gastric cancer (Ma et al., 2001) and leukemia (Li et al., 2009), prostate cancer (Kanazawa et al., 2003) and hepatoma (Hsu et al., 2005). However, no obvious inhibition effect of IQ on DNR efflux was observed, as the efflux-in-IQ curves were similar to the efflux-in-medium curves (see Figure 5a).

Figure 5a shows the typical curves of DNR efflux among results obtained from multiple individual cells. The typical curves represent the cluster of the curves for most cells, as opposed to some outliers, see Figure 5b-d. Even in the same cluster, some cellular variations were observed. For instance, Figure 5b shows the variations in the cluster of the drug-resistant cell line (CEM/VLB) and that of the CEM wild-type cell line (CEM/wt). Although it can be comfortably inferred that there is a lower drug retention in the CEM/VLB cells than in the CEM/WT cells, which was attributed to the overexpressed Pgp pumps in the CEM/VLB cells (Higgins, 2007), there are still many variations observed in both clusters. It can be observed that some curves of CEM/VLB cells are even close to those of the CEM/WT cells, indicating some CEM/VLB cells have more drug retention, which is likely due to less Pgp pump activities.

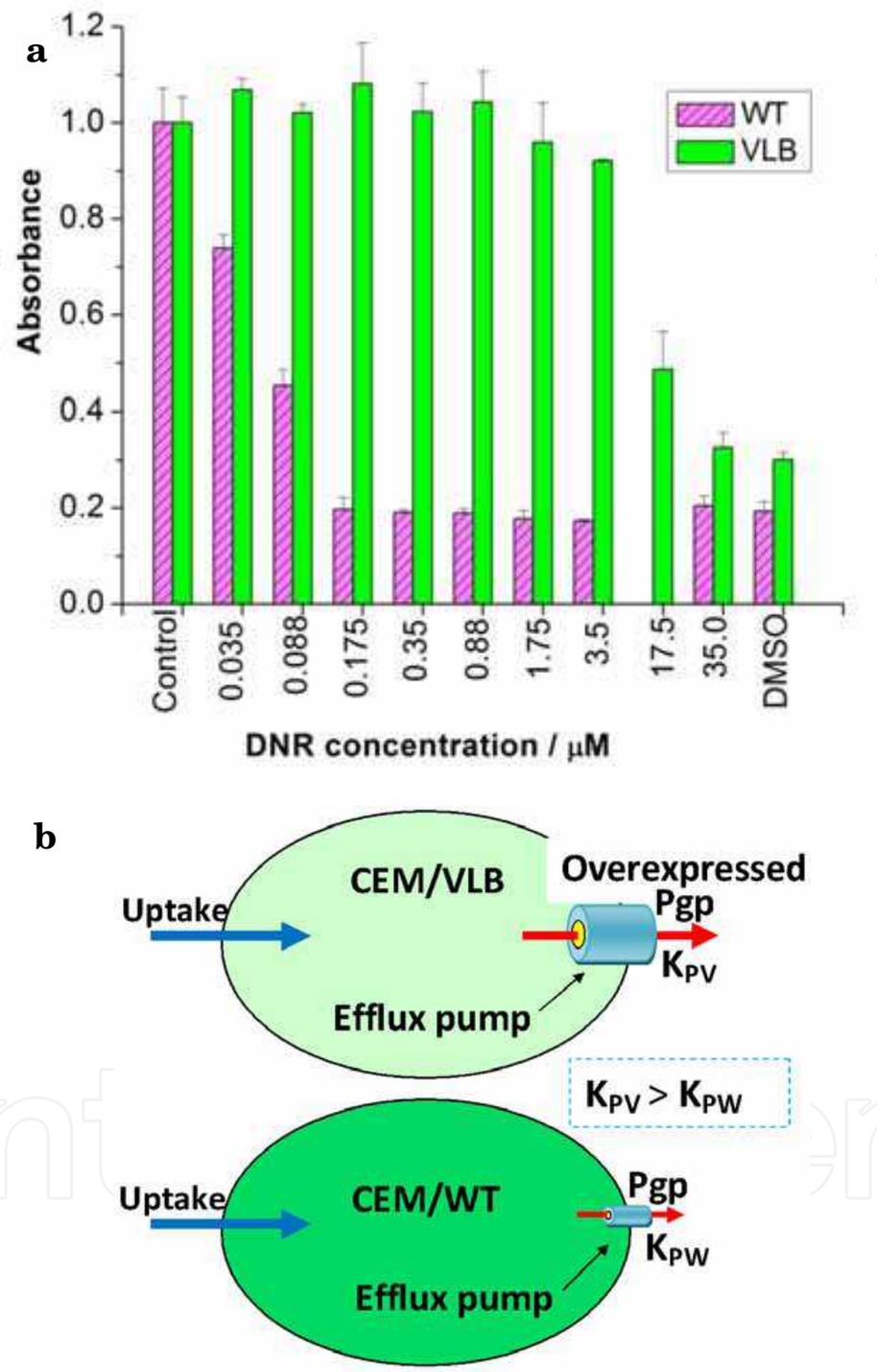

Fig. 4. (a) Cytotoxicity assay to show the different drug sensitivities of WT and VLB cells toward DNR. (b) A drug accumulation model to describe the higher drug sensitivities (or lower drug resistance) of the WT cells, as compared to the VLB cells. K_{PV} and K_{PW} are the drug efflux rates in VLB and WT cells, respectively. Reprinted with permission from Royal Society of Chemistry(Li et al., 2011)

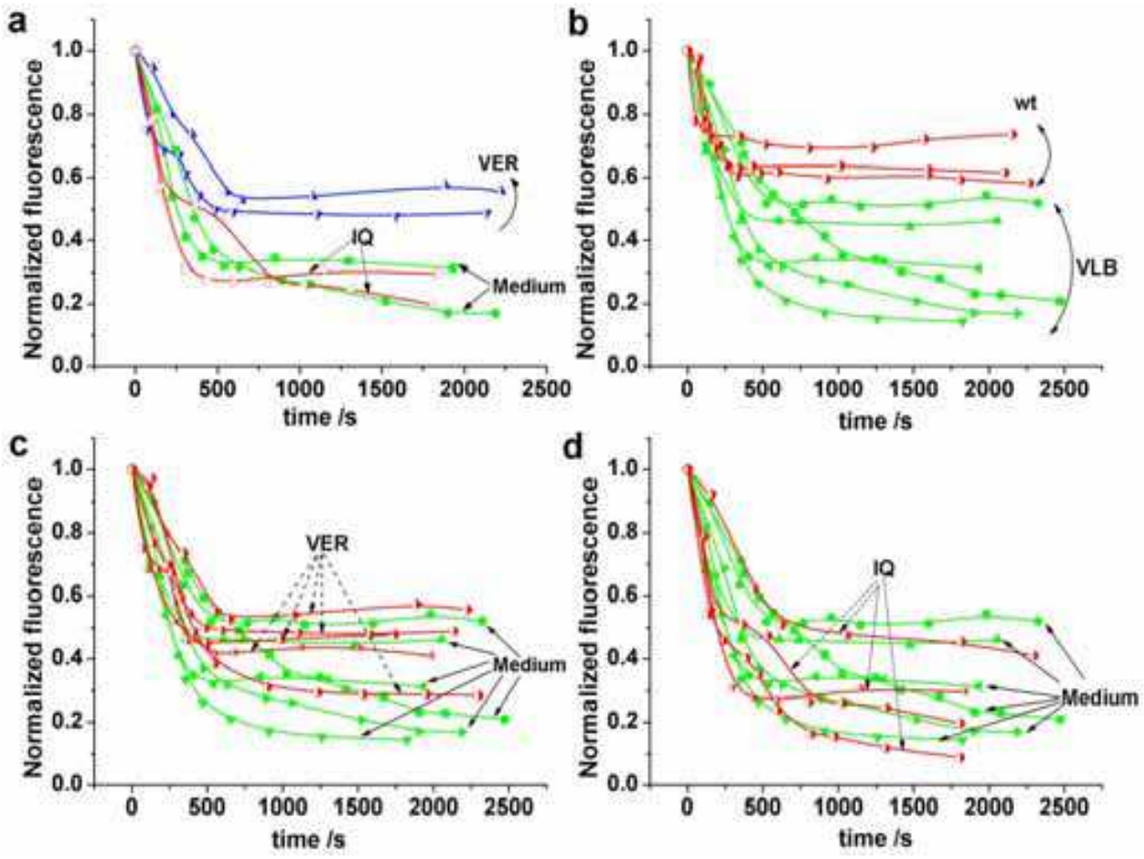

Fig. 5. Modulation of DNR efflux by VER and IQ studied by DISCA in a microchip. (a) The typical curves of DNR efflux of CEM/VLB cells in the medium (green, solid symbols), in 50 μM VER (blue, half-filled symbols) and 100 μM IQ (red, hollow symbols). (b) Comparison of DNR efflux in medium between CEM/WT (red, half-filled symbols) and CEM/VLB (green, solid symbols) cells. (c) The effect of VER (red, half-filled symbols in panel) on the DNR efflux in CEM/VLB cells. (d) The effect of IQ (red, half-filled symbols in panel) on the DNR efflux in CEM/VLB cells. DNR, 35 μM. IQ is isoliquiritigenin; VER is verapamil; ART is sodium artesunate. Reprinted with permission from American Chemical Society (Li et al., 2008)

In the cases of drug efflux in VER and in IQ, the MDR reversal effects from these compounds cannot be concluded due to the enormous cell variations in the efflux-in-VER cluster, and in the efflux-in-IQ cluster, as shown in Figure 5c and 5d, respectively. Although it is well known that verapamil (VER) could inhibit the MDR efflux and result in more drug retention (Akiyama et al., 1988; Wang et al., 2000), this positive effect of MDR reversal cannot be verified in Figure 5c as some efflux-in-VER curves are mixed with the efflux-in-medium curves. Since the effect of IQ on MDR reversal is unknown, it is difficult to draw any conclusion when we examine Figure 5d. Under this situation, we selected the typical curves in each of the 3 cases (shown in Figure 5a) as obtained from many single-cell experiments, and tentatively concluded that there is a MDR reversal effect by VER, but not by IQ.

More single-cell measurements could help the data interpretation and this is one of the reasons why conventional FACS requires a large number of cells to achieve reliable results (Wang et al., 2005). Nevertheless, it may not be possible to conduct many measurements in

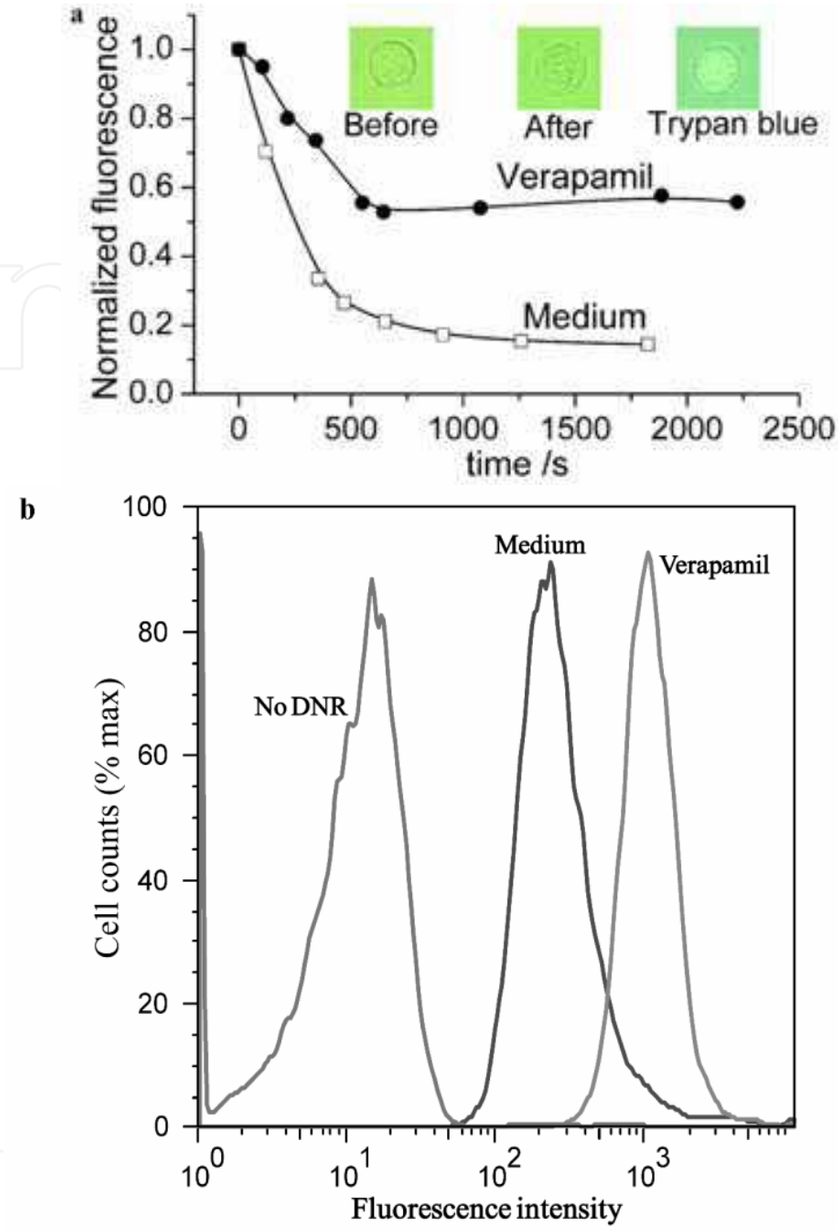

Fig. 6. Modulation of 50 μM verapamil (VER) on DNR efflux of CEM/VLB cells studied by SASCA and confirmed by flow cytometry. (a) SASCA method used to study the effect of MDR reversal by VER on one and the same CEM/VLB cell. The fluorescence intensities of DNR efflux in medium and in VER have been normalized for easy comparison. The insets show the cell morphologies before and after the experiment, and after trypan blue treatment. (b) Flow cytometry study of the modulation of DNR efflux in CEM/VLB cells by VER. The histograms represent the normalized percentage of cell counts plotted against the fluorescent intensity expressed as log relative fluorescence. The histograms depict, from left to right, the cells without DNR accumulation; the cells with DNR efflux in medium alone; and the cells with DNR efflux in VER. DNR, 35 μM. Reprinted with permission from American Chemical Society (Li et al., 2008)

the case of cancer stem cells because of the limited number of cells available. It is because one drawback of using DISCA for the MDR efflux study is the inevitable variations in cellular properties, such as the MDR activities. In a worse case scenario: if the control cell has a lower drug efflux ability (e.g. the highest efflux-in-medium curve in Figure 5c), and the test cell has a greater drug efflux ability (e.g. the lowest efflux-in-VER curve in Figure 5c), the MDR reversal effect of the candidate compound will not be obvious, leading to a false negative conclusion.

3.3 Same-single-cell analysis (SASCA) for drug efflux study in a microfluidic chip

In order to minimize cellular variations, we conduct the drug efflux study in which the same cell is employed as the control cell as well as the test cell. This analysis is thus called same-single-cell analysis (SASCA). This demands the single cell to be retained long enough during the course of the drug efflux study, and is achievable by the cell retention ability of the microfluidic chip. The schematic diagram in Figure 3b shows the concept of the SASCA, in which 2 cycles of DNR accumulation and efflux steps are conducted on the same single cell (e.g Cell 3). As depicted in the inset of Figure 3b, the 2 efflux curves (Es3 vs Es3′) obtained from one and the same cell are compared.

Since the well known effect of MDR reversal of verapamil (VER) cannot be verified by DISCA as shown in Figure 5c, we conduct SASCA to verify this effect. Figure 6a shows that there is indeed a greater DNR retention when the cell efflux was conducted on the same cell in the presence of VER and so it is clear that this well known modulator has reversed the DNR efflux process. More SASCA data confirm the same positive result of MDR reversal by VER (see Table 1).

Conventional flow cytometry was also performed to confirm the effect of VER. From Figure 6b, it is found that the fluorescent intensity (plotted as the x-axis), which indicates the intracellular DNR retention, is greater when the drug efflux study is conducted in VER than in the cell medium alone, corroborating the microfluidic results. In the flow cytometry experiment, during the drug accumulation and efflux procedures (a total of 60 min.) and before data collection, no cellular information is collected. But, in SASCA, the full profile of the drug transport in the same single cell is recorded even during drug accumulation and efflux. In addition, this approach has provided information about the cell morphology, which can be seen in the cell images in Figure 6a inset, showing little cell shape changes, and non-staining by trypan blue. This data suggested that the cell was still viable, indicating not only that the drug-resistant cell was not killed by DNR due to substantial drug efflux, but also that the microfluidic method was robust enough for long-term cell measurement. The cell images could also be useful in documentation and data interpretation of the MDR reversal response. Furthermore, SASCA can comfortably measure one cell selected from a small cell population of ~100, in contrast to flow cytometry that requires ~100,000 cells to achieve high yield in data collection. A full comparison between flow cytometry and SASCA, in terms of experimental time, information content, throughput and automation, has been previously reported (Li et al., 2008).

In a similar manner, the effect of IQ on DNR efflux was studied. It is clear in Figure 7a that IQ did not result in a greater DNR retention, and so IQ was ruled out as a MDR modulator candidate. Again, the use of the same cell as both the control and test cells in SASCA rules out the variations among different cells, and assists in a conclusive data interpretation. More experiments on IQ (see Table 1) were conducted, and the same observation (no MDR reversal effect by IQ) was achieved. The microchip data are also consistent with the histograms

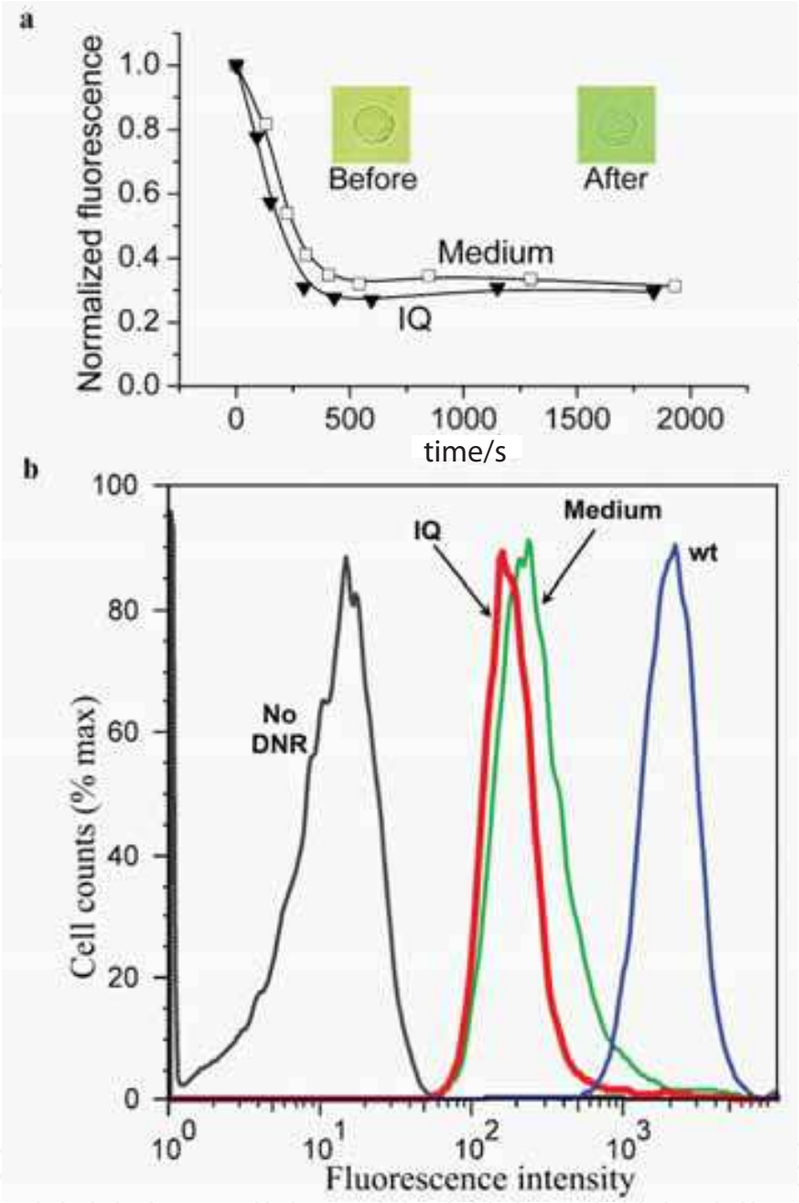

Fig. 7. Effect of IQ on DNR efflux of CEM/VLB cells studied by SASCA and confirmed by flow cytometry. (a) Effect of 100 μM IQ on MDR reversal studied on one and the same CEM/VLB cell. Other conditions are the same as Figure 6a. (b) Flow cytometry study of DNR efflux in CEM cells as treated by IQ. The histograms represent, from left to right, the CEM/VLB cells without DNR accumulation; the CEM/VLB cells with DNR efflux in IQ (100 μM); the CEM/VLB cells with efflux in medium alone; and the CEM/WT cells with DNR efflux in medium alone. Others conditions for flow cytometry are the same as Figure 6b. Reprinted with permission from American Chemical Society (Li et al., 2008)

obtained by conventional flow cytometry (Figure 7b), which shows the CEM/VLB cells have a similar DNR retention in IQ as in medium alone, while DNR retention in CEM/WT cells is greater than that of the CEM/VLB cells. Similar to the VER experiment, the flow cytometry

data did not give more information than SASCA regarding the conclusion of the IQ effect, although the histograms provide valuable information about cell distribution, which may be important in applications such as the cell-cycle study.

	Verapamil (VER)			Isoliquiritigenin (IQ)			Artesunate (ART)			
	Cell 1	Cell 2	Cell 3	Cell 4	Cell 5	Cell 6	Cell 7	Cell 8	Cell 9	Cell 10
P_d (%)	42.2	28.8	55.7	29.6	45.3	8.8	19.3	35.7	68.8	66.1
P_c (%)	31.7	17.2	14.4	31.7	40.8	14.4	14.9	10.8	47.6	38.0
ΔP (%)	10.5	11.6	41.3	-2.1	4.5	-5.6	4.4	24.9	21.2	28.1
Average ΔP (%)		21±17			-1.1±5.1			19.7±10.6		
$R_p = P_d / P_c$	1.33	1.67	3.87	0.93	1.11	0.61	1.30	3.31	1.45	1.74
Average R_p		2.3 ±1.4			0.88 ±0.25			1.95 ±0.92		
G_p		3.83±0.86			0.72±0.21			1.39		

Table 1. DNR efflux in CEM/VLB cells as modulated by IQ, VER and ART using SASCA. See eqs (1-3) for the definitions of P_d, P_c, ΔP, R_p, and G_p. Reprinted with permission from American Chemical Society (Li et al., 2008)

To quantitatively evaluate the MDR modulations or MDR reversal effects of various drug candidates, we define 2 parameters, ΔP and R_p, as follows:

$$\Delta P = P_d - P_c \quad (1)$$

$$R_p = P_d / P_c \quad (2)$$

where P_d and P_c are the DNR retention percentages in the MDR modulator solution and in the medium alone (control), respectively, see Figure 3b inset.
In flow cytometry, the fluorescence geometric mean ratio, G_p, is used, as defined in equation 3 (Medeiros et al., 2007) (Wang et al., 2000).

$$G_p = G_d / G_c \quad (3)$$

where G_d and G_c are the fluorescence geometric means in the MDR modulator solution and in the medium (control), respectively.
ΔP gives the DNR retention percentages that the drug candidate can reverse, i.e. the larger the ΔP value, the greater is the drug's MDR reversal. On the other hand, a negative ΔP value means that the drug candidate potentiates the drug efflux, resulting in less drug retention. R_p is defined for comparison with the data obtained from the flow cytometry method (i.e. G_p). The higher is the R_p value above 1, the greater is the MDR inhibition effect; R_p =1 means that the drug candidate does not have any MDR modulation effect. If R_p is less than 1, it means the drug candidate potentiates the drug efflux.
Several experiments of 50 μM VER by SASCA show that the highest values of ΔP and R_p are 41.3 and 3.87, respectively (Table 1), indicating that Cell 3 would have the greatest MDR reversal effect. This demonstrates the capability of SASCA to evaluate the different cellular abilities in response to drug efflux modulation. To compare with the flow cytometry data, the averaged values were used, and the average ΔP and R_p for VER (50 μM) are 21±17% and 2.3±1.4 (n=3), respectively (Table 1). The values of ΔP and R_p for IQ (100 μM) are similarly compared, and they are -1.1±5.1% and 0.88 ±0.25 (n=3), respectively. The R_p values (2.3±1.4

and 0.88±0.25) for VER and IQ are similar to the G_p values (3.83±0.86 and 0.72±0.21) obtained from flow cytometry data.

The difference in R_p and G_p values may result from the differences between these two measurement methods, and the amount of tested cells, but this does not affect the conclusion of MDR modulation in both cases. Although R_p is defined for comparison with the results obtained from the flow cytometry method (e.g. G_p), we believe ΔP should be used in evaluating the drug candidate's MDR reversal effect in SASCA since the P_d and P_c values have already been normalized into the percentages. Moreover, R_p may be substantially affected by the denominator (P_c), especially when the value of P_c is very small.

The MDR modulation effect of another herbal ingredient, sodium artesunate (ART) was also studied. ART, which was derived from 'Qinghao', was first discovered as an anti-malarial drug (Dai and Chen, 1999), and subsequently found to have anti-cancer property (Wang et al., 2002). Figure 8a shows that the DNR efflux is reversed in the presence of ART, as compared with the efflux in the cell medium (medium 1, before ART). In order to confirm this finding, a second efflux step in the medium (medium 2) was conducted after the MDR reversal by ART. It was found that the efflux-in-medium curve in the second case was consistent with that in the first, thus confirming the finding that the MDR modulation effect of ART was genuine. More same-single-cell experiments also confirmed the effect of ART (300 μg/mL) on MDR efflux, as shown by the mean values of ΔP and R_p, which are 19.7±10.6% and 1.95 ±0.92, respectively (see Table 1). It has been reported that ART (60 μg/mL) significantly increased DNR accumulation in the MRP1-expressing cells, but not in the MDR1-expressing CEM cell line (Efferth et al., 2002). We discovered that when ART was more concentrated than 200 μg/mL, it produced a beneficial MDR inhibition effect, consistent with the flow cytometry data (Figure 8b). No inhibition effect on MDR efflux was observed in lower concentrations of ART (100 μg/mL).

3.4 Simpler, faster, and more reliable method of microfluidic same-single-cell analysis

The study of multidrug resistance based on drug efflux is fairly complicated because it involves multiple cycles of drug uptake and drug efflux, and each assay is time-consuming. In addition, the time period between the two drug efflux processes (i.e. test and control or $t_{e1} + t_r + t_{a2}$,), as shown in Figure 9a, might cause slight differences in the cellular health status or Pgp activities. Although multiple controls can be adapted to confirm cell status as we reported previously (Li et al., 2008), it complicates the assay process. To overcome these problems and work toward an 'identical' control, we are reporting a new microfluidic SASCA approach for the study of MDR modulation by monitoring drug accumulation in single cells. Based on the same concept of SASCA, this new approach is simpler, faster and more reliable for MDR study by investigating drug accumulation, instead of drug efflux.

As illustrated in the Figure 9b inset, during the drug accumulation stage in the presence of DNR, the drug uptake process and the drug efflux process by Pgp pumps occur simultaneously. In contrast to WT cells, more DNR is pumped out of MDR cells, leading to low drug accumulation in these cells. But when the MDR cells' Pgp pumps are inhibited by a MDR modulator compound (e.g., VER), less DNR is pumped out, leading to a higher intracellular drug accumulation (i.e., the MDR reversal effect). Therefore, we can choose to measure DNR accumulation in order to determine whether a compound has the MDR reversal effect, instead of the time-consuming measurement of the DNR efflux process (Li et al., 2008). We call this approach SASCA-A to differentiate it from the previous approach of same-single-cell analysis, termed as SASCA (Li et al., 2008).

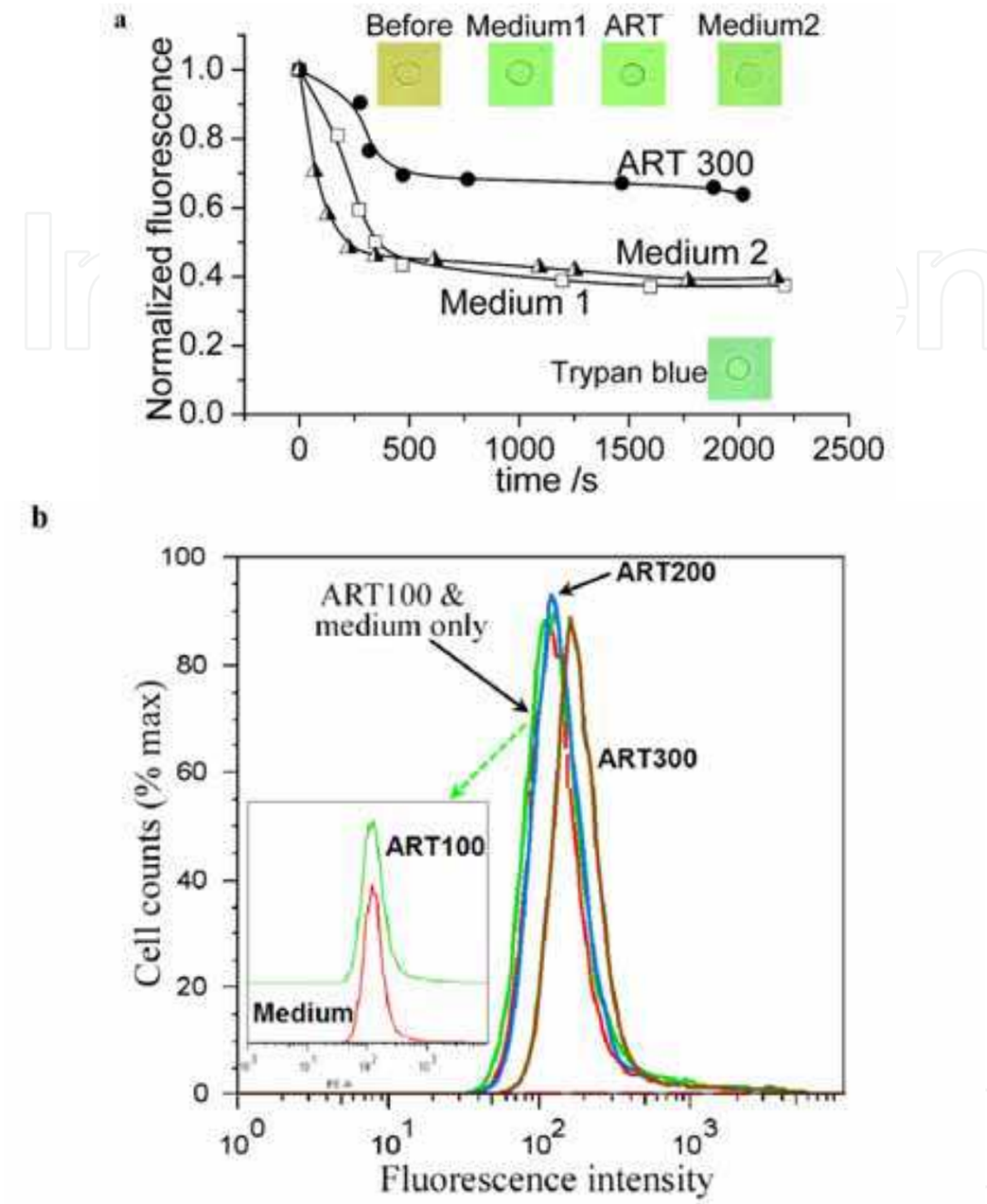

Fig. 8. Modulation of ART on DNR efflux of CEM/VLB cells as studied by SASCA (a) and confirmed by flow cytometry (b). (a) Effect of MDR reversal by ART (300 μg/mL) studied by SASCA on one and the same CEM/VLB cell in a microfluidic chip. A second efflux in medium (Medium 2) confirmed that the effect of 300 μg/mL ART (ART300) was genuine after the first efflux in medium (Medium 1). Both efflux steps in medium alone were used as control experiments. Other conditions are the same as Figure 6a. In (b), flow cytometry revealed the effect of artesunate (100, 200, 300 μg/mL) on DNR efflux in CEM/VLB cells. The histograms from the medium alone and 100 μg/mL ART are offset vertically and shown in the inset to provide greater detail. Others conditions for flow cytometry are the same as Figure 6b. Reprinted with permission from American Chemical Society (Li et al., 2008)

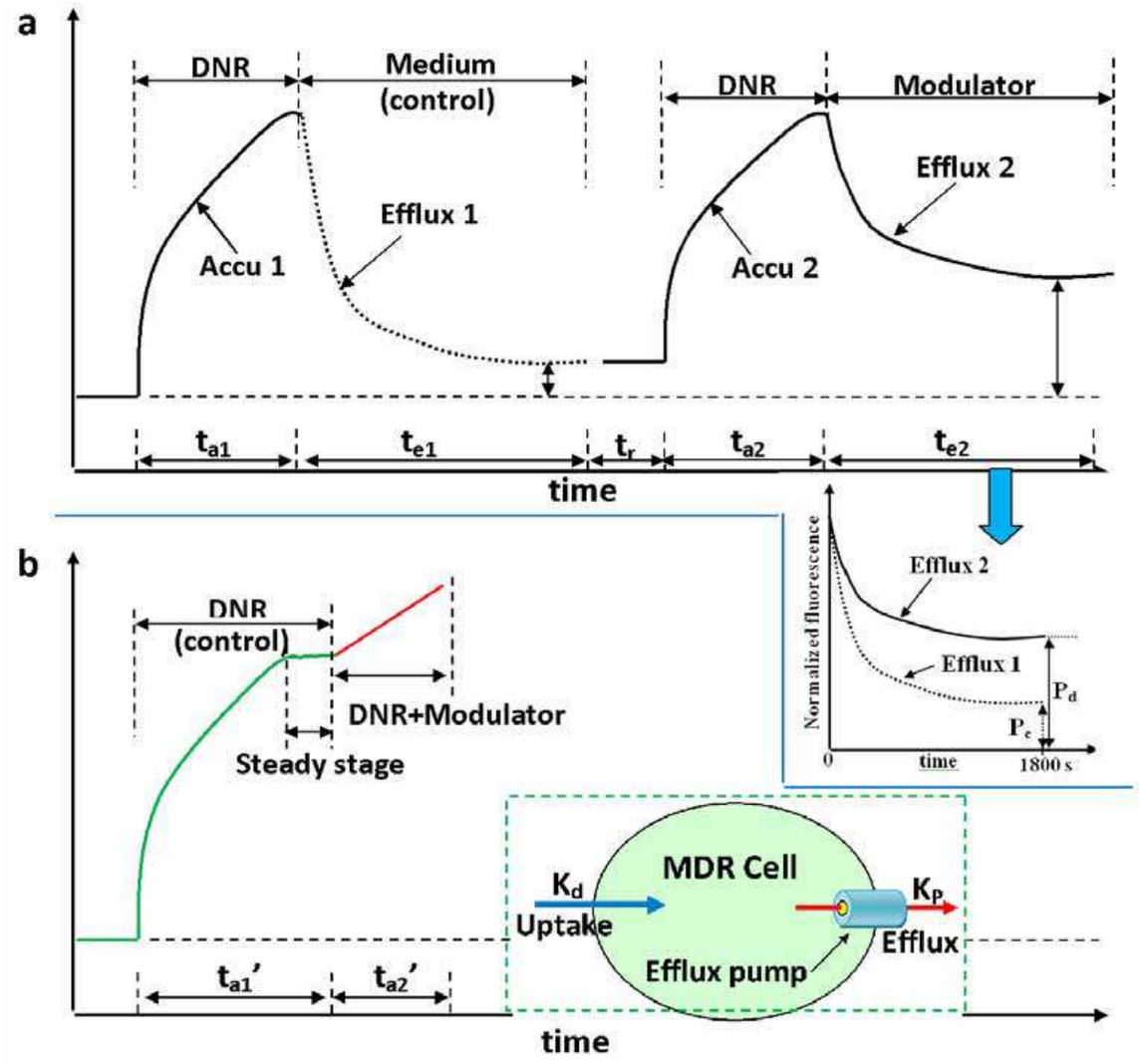

Fig. 9. The schematic illustration of two SASCA approaches for single-cell multidrug resistance study (a) by a microfluidic method measuring drug efflux process and (b) by a new approach via investigating drug accumulation. The inset depicts a mathematical model to describe the kinetics of drug accumulation, with K_d and K_p representing the drug uptake rate and drug efflux rate, respectively. Reprinted with permission from Royal Society of Chemistry (Li et al., 2011)

In the SASCA-A experiment, we used a lower concentration of DNR (e.g., 8.8 μM) to minimize cytotoxic effect on cells. It was found that the accumulation was initially fast, then it reached a relatively 'steady' state (after 470 s as seen in Curve 3 in Figure 10). This showed a balance of the drug uptake and efflux processes, as previously observed (Ren and Wei, 2004)(Wang et al., 2000). It was only when the DNR concentration was low enough and the accumulation was relatively slow that the 'steady' accumulation stage was obvious. During this 'steady' state, if an MDR inhibitor-containing DNR solution is applied (see Figure 9b and 10), the MDR modulation will tip the balance at this 'steady' state, and the drug accumulation rate will increase instantly. This is shown by the abrupt slope change in the

curve (see Figure 9b and 10). This provides us a simple and fast means to monitor MDR modulation using this SASCA-A method, without a long waiting period which is inevitable in the previous SASCA method (Li et al., 2008).

Figure 10 shows an obvious slope transition in the drug accumulation curve when a VER–containing DNR solution was applied to the cell at 1370 s (Curve 3). The slope transition indicates a MDR reversal effect in which there is a faster DNR accumulation as compared to the 'steady' state before VER was added. Thus, the MDR reversal effect of VER can easily be determined by the new approach of microfluidic SASCA-A. However, when an IQ-containing DNR solution was added, no obvious slope transition was observed (see Curve 2). This was similar to the negative control when only DNR (without MDR inhibitors) was applied (at 1562 s in Curve 1), which indicated that IQ did not have MDR reversal effect on CEM cells. More SASCA data confirmed the different reversal effects from VER and IQ, as listed in Table 2. The SASCA-A method can readily conclude the effects of not only VER but also IQ, directly on the same single cell, by minimizing the cellular variations among different single cells. The effects of VER and IQ were further confirmed by the conventional technique of flow cytometry (data not shown).

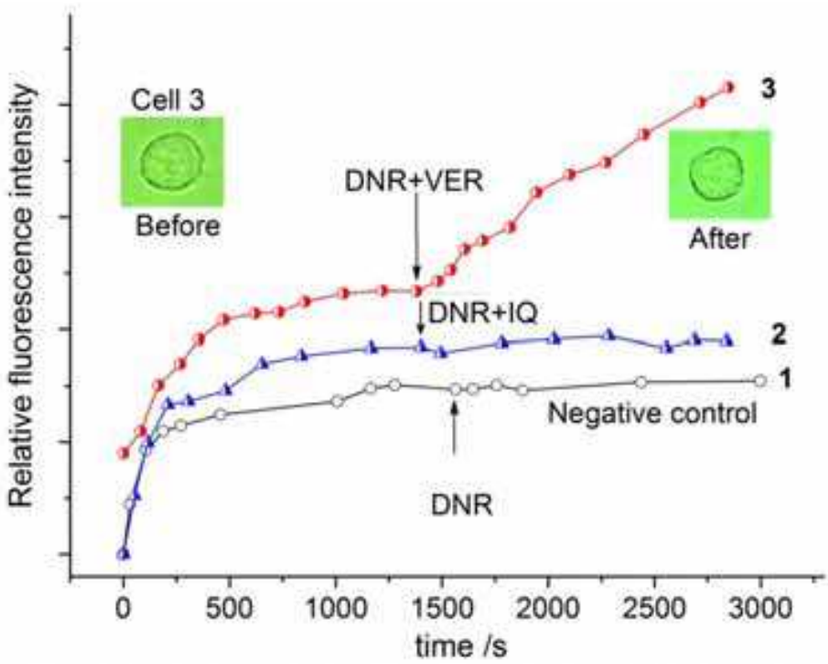

Fig. 10. MDR modulations from VER and IQ in CEM/VLB cells by the new approach of the same-single-cell analysis of drug accumulation (SASCA-A). DNR solutions (8.8 μM) in the presence of VER (50 μM) and IQ (100 μM) were applied to cells at 1370 s (Curve 3) and at 1402 s (Curve 2), respectively. In Curve 1, 8.8 μM DNR in the absence of MDR modulators was added at 1562 s as a negative control. The relative fluorescence intensities have been offset for clarity. The inset shows the images of the cells before and after the VER experiment. Reprinted with permission from Royal Society of Chemistry (Li et al., 2011)

In a similar manner, this microfluidic SASCA-A approach was applied to study the effect of PSC 833 on MDR modulation. PSC 833 (Valspodar, a non-immunosuppressive cyclosporin D derivative) is a less toxic Pgp inhibitor (Thomas and Coley, 2003). As shown in Figure 11,

a slope transition was observed as soon as 3 μM PSC 833 in a DNR solution was applied to the cell at 1458 s (see Curve 2), indicating a faster drug accumulation due to the inhibition of Pgp pumps by PSC 833. More same-single-cell experiments also confirmed the MDR reversal effect of PSC 833 on drug accumulation in MDR cancer cells. This is consistent with previous reports that PSC 833 can inhibit Pgp pumps and improve the chemotherapy response (Warmann et al., 2002). As a control, when the same PSC 833 solution was applied to CEM/WT cells (at 1368 s on Curve 3), no obvious slope transition occurred and the drug accumulation in the cells still increased linearly with the same slope as before. This implied

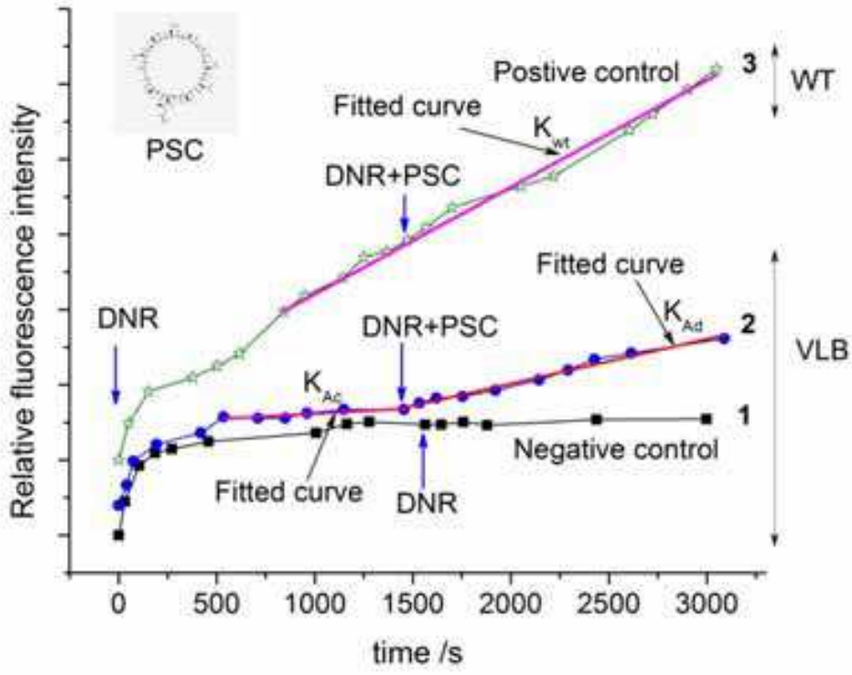

Fig. 11. MDR modulations from PSC 833 in CEM cells by the microfluidic approach of SASCA-A. DNR solutions (8.8 μM) in the presence and absence of 3.0 μM PSC 833 were applied to CEM/VLB cells at 1458 s in Curve 2 and at 1562 s in Curve 1, respectively. In Curve 3, a DNR solution (8.8 μM) in the presence of 3.0 μM PSC 833 was applied to a CEM/WT cell at 1465 s. The relative fluorescence intensities have been offset for easy comparison. The different segments of Curve 2 and Curve 3 have been linearly fitted and shown as straight lines along the curves. K_{Ac} and K_{Ad} are the slopes of fitted lines before and after applying drug modulators in CEM/VLB cells, and K_{wt} is the slope of the fitted line in CEM/WT cells. Reprinted with permission from Royal Society of Chemistry (Li et al., 2011)

that the MDR modulator did not have any reversal effect on the drug accumulation in CEM/WT cells, as were similarly observed in previous reports (Hu et al., 1990). During the drug accumulation in WT cells as seen in Curve 3, no obvious 'steady' state was observed, and yet the accumulation rate was fairly constant after 838 s. As time went on, there was an increasingly greater deviation in the amount of drug accumulation between WT cells (Curve 3) and drug-resistant cells (Curve 1). Accordingly, the SASCA-A approach cannot only readily identify MDR modulators, but can also clearly distinguish CEM sensitive cells from MDR cells. This method might be used to distinguish MDR cells or cancer stem cells from a population of cells.

To quantitatively evaluate the MDR modulations or MDR reversal effects of various drug candidates using the SASCA-A method, two parameters have been defined, namely, the ratio of drug accumulation rates (denoted as R_A), and the MDR reversal percentage ($\Delta R_A\%$), as follows:

$$R_A = \frac{K_{AD}}{K_{AC}} \tag{4}$$

$$\Delta R_A\% = \frac{K_{AD} - K_{AC}}{K_{wt}} \tag{5}$$

where K_{Ad} and K_{Ac} are the slopes of the linearly fitted lines on the drug accumulation curves of the CEM/VLB cells in the presence of drug plus MDR modulators (modulators + DNR) and in the absence of MDR modulators (DNR only), respectively; K_{wt} is the slope of the fitted line on the curve of the CEM/WT cell.

In this way, R_A indicates how much a MDR modulator affects the drug accumulation in a MDR cell. Therefore, the greater R_A is, the stronger the reversal effect of MDR modulators will be. Since R_A does not reveal how close the MDR reversal of the VLB cell is to the drug accumulations in the WT cell, we have also defined $\Delta R_A\%$. Based on these two equations, the values of R_A and $\Delta R_A\%$ were calculated and listed in Table 2. Both average values of R_A and $\Delta R_A\%$ confirm the positive MDR reversal effects by VER and PSC 833, but not by IQ. The average values of $\Delta R_A\%$ of VER, IQ, and PSC 833 are 57.4, -0.1, and 29.5, respectively, showing that 50 μM VER has a greater MDR reversal effect as compared to 3 μM PSC 833. From Table 2, we also found that different cells responded to MDR modulators differently. The values of $\Delta R_A\%$ of VER on cell 1, 2, and 3 are 67.0%, 52.7%, and 52.3%, respectively. Cell 1 shows the highest response on the MDR reversal effect from VER among the cells tested in this work. This kind of cellular heterogeneity in MDR modulation was also observed in previous reports (Li et al., 2008).

	verapamil (VER)			isoliquiritigenin (IQ)			PSC 833 (PSC)		
	Cell 1	Cell 2	Cell 3	Cell 4	Cell 5	Cell 6	Cell 7	Cell 8	Cell 9
R_A	7.2	9.1	27.5	0.9	0.9	1.1	4.2	16.5	4.5
Average R_A	14.6±11.0			1.0±0.1			8.4±7.0		
K_{wt}	0.0081±0.0005								
$\Delta R_A\%$	67.0	52.7	52.3	-0.7	-0.6	1.0	27.9	33.8	26.9
Average $\Delta R_A\%$	57.4±8.4			-0.1±1.0			29.5±3.7		

Table 2. DNR accumulation in CEM/VLB cells as modulated by VER (50 μM), IQ (100 μM), and PSC833 (3 μM) using SASCA-A. For notations, see Figure 11 and eqn (4-5). Reprinted with permission from Royal Society of Chemistry (Li et al., 2011)

3.5 Dynamics of drug accumulation in MDR cells

We believe the understanding of drug accumulation dynamics in MDR cells will benefit the design and exploitation of novel MDR inhibitors. Therefore, we have also developed a mathematical model to describe the process of drug accumulation. As shown in the Figure 9b inset, the drug accumulation rate is determined by the drug uptake process as well as the drug efflux process by Pgp pumps. Assuming that the drug uptake is by passive diffusion

and the drug efflux is controlled by an enzymatic process based on the Michaelis-Menten equation (Peng and Li, 2004, Agarwal et al., 2007), we developed the following equation to describe the drug accumulation dynamics (See the reference (Li et al., 2011) for the derivation).

$$\frac{dc}{dt} = \frac{A}{V} \times \left(\underbrace{D \times \frac{c_{out} - c_{in}}{x}}_{(a)} - \underbrace{\frac{v_{\max} \times c_{in}}{K_m + c_{in}}}_{(b)} \right) \tag{6}$$

where C is the concentration of DNR; t is the time; C_{out} and C_{in} are the extracellular and intracellular DNR concentrations, respectively; D is the diffusion coefficient; A is the cell surface area; V is the cell volume; x is the cell membrane thickness; and $v_{\max}$ and K_{m} are the maximum rate and the Michaelis-Menten constant, respectively, in the Michaelis-Menten equation for the drug efflux process.

From this equation, we find the initial drug accumulation is dominated by the drug uptake process when there is a large gradient (C_{out}-C_{in})/x between extracellular and intracellular DNR concentrations. Due to this large gradient, the initial drug accumulation rate is very fast, as shown by Curve 1 in Figure 11 (before 100 s). When the gradient across the cell membrane becomes smaller, the drug uptake becomes slower (see part (a) of eqn (6)). The drug efflux process begins to play a significant role in the dynamics of the drug accumulation process (see part (b) in eqn (6)). When the drug uptake rate is close to the drug efflux rate, that is, part (a) is similar to part (b) in eqn (6), it will reach a 'steady' state, as shown by the part of curve 1 (Figure 11) after 450 s. However, when a MDR modulator is applied, it will bind to Pgp, and inhibit the drug efflux pump, leading to a decrease of the maximum efflux rate ($v_{\max}$) shown in eqn (6). Accordingly, the drug uptake process again dominates, as shown by the upward slope transition in the drug accumulation (see Curve 2 in Figure 11). Therefore, the data obtained from the SASCA-A method can help us to understand the drug accumulation in multidrug resistance. Further work about the simulation of the various processes involved in multidrug resistance is underway. A note of caution: the cellular kinetic response can be misinterpreted by averaging the data obtained from bulk analysis (Di Carlo and Lee, 2006).

4. Conclusion

The same-single-cell analysis conducted in a microfluidic chip has demonstrated the advantages in identifying MDR modulators, and in quantifying the MDR reversal effect of drug candidates during the drug efflux stage based on the defined parameter of ΔP. It has been demonstrated that SASCA is superior to DISCA by ruling out the difference in MDR activities among different cells and presenting a conclusive result about the effect of MDR modulators by using the same cell as both the test and the control cell.

SASCA is also compared with the conventional flow cytometry method in the study of MDR modulator candidates. The time needed to conduct SASCA is shorter than flow cytometry, and the microfluidic operation will become less tedious after automation in cell manipulation and fluorescent data collection. Moreover, the microfluidic SASCA method can provide time-dependent drug transport kinetics and cell morphological information, and only a small amount of cells are needed to confirm the findings. Therefore, this technique may have significant potential for investigating drug resistance in minor cell subpopulations (e.g. cancer stem cells) that may be the key determinant of clinical response to chemotherapy.

In addition, this microchip-based method, SASCA, is envisioned for clinical use as a companion diagnostics method, e.g. to check the MDR profile and drug responses so as to identify personalized drugs before patient treatment starts. This is an important step in determining the drug efficacy in individual patients. This approach will be even more robust if multiple parallel channels/structures are used to improve throughput (Di Carlo et al., 2006)(Faley et al., 2008). Moreover, the time-dependent data from SASCA can help us to understand the kinetics and mechanism of drug accumulation or efflux in MDR cancer cells.
Compared to the SASCA approach for the MDR modulation study in the drug efflux stage (Li et al., 2008), the new method—microfluidic SASCA-A has four significant advantages. (1) It is simpler; as illustrated in Figure 9, it does not need multiple drug accumulation and drug efflux stages as used in the previous SASCA method. (2) It is faster; a typical SASCA-A experiment could be finished within 2200 s ($t_{a1}'+t_{a2}'$ in Figure 9b). That is about one fourth of the time used in the previous SASCA experiments ($t_{a1}+t_{e1}+t_r+t_{a2}+t_{e2}$). As a more efficient assay method, this improves the throughput of MDR assays. (3) SASCA-A provides more 'identical' and reliable controls. Here, the previous SASCA has two limitations. First, the previous SASCA needs a longer measurement time. Long term exposure to cytotoxic drugs is detrimental to cells because the cell status or health conditions may change over time. To make sure the cell still have similar conditions, a second control experiment could be conducted, as we reported previously in testing ART (Li et al., 2008). Nevertheless, this dual control experiment makes the assay more complicated, and consumes more time. Secondly, there is a time interval of ~ 3700 s ($t_{e1}+t_r+t_{a1}$ in Figure 9a) between the two efflux stages in the previous SASCA approach; that is, the two efflux stages start at different life time points of a cell. Even though these points refer to the same cell, they are still not true identical controls. In terms of Pgp, which has been the most studied drug efflux protein (Perez-Tomas, 2006) (Gillet et al., 2007)(Davey et al., 1996), research shows that after the drug molecules bind to the transmembrane domains of the protein, the ATP-binding domains are activated and the drug molecules are then transported out of the cell by a major conformational change of Pgp via an enzymatic process (Perez-Tomas, 2006)(Higgins, 2007). During this time interval of ~ 1 h, any change in the enzymatic process might cause changes in the drug efflux abilities of Pgp pumps.
Considering these two limitations from the previous SASCA method, SASCA-A takes less time and it compares the time points just before MDR modulator tests. Therefore, SASCA-A has a more 'identical' and reliable control than SASCA. (4) SASCA-A may be more accurate in representing the patient's cells during cancer chemotherapy in which the cancer patient is exposed to a continuous drug infusion for a defined period of time.
In conclusion, it is found that it is less time-consuming to evaluate MDR reversal effects of drug candidates by studying the drug accumulation stage than the efflux stage using SASCA. Having said that, in the investigation of MDR dynamics, it might be less complex to study the drug efflux stage than to study the drug accumulation stage. It is because in the former case, only the drug efflux process is involved, but in the latter case, both drug uptake and efflux processes should be accounted for. Therefore, the combination of studying both stages will likely provide insight for the overall mechanism of multidrug resistance, especially when associated with cancer stem cells.

5. Acknowledgment

Financial support from Natural Science and Engineering Research Council (NSERC) of Canada is acknowledged. We are also grateful to Dr. Victor Ling and Dr, Donna Hogge (BC

Cancer Research Center, Vancouver, Canada) for providing PSC 833 and useful suggestions, to Dr. Thomas Efferth (German Cancer Research Centre, Heidelberg, Germany) for providing sodium artesunate, and to Dr. Jamie Scott for the use of the FACS instrument. The author XJL appreciates the support from NSERC of Canada for the Postdoctoral Fellowship.

6. References

Agarwal, S., R. Jain, D. Pal & A. K. Mitra (2007). Functional characterization of peptide transporters in MDCKII-MDR1 cell line as a model for oral absorption studies. *Int. J Pharm.*, Vol.332, No.1-2, pp.147-52, ISSN 0378-5173 (Print) 0378-5173 (Linking).

Akiyama, S. I., M. M. Cornwell, M. Kuwano, I. Pastan & M. M. Gottesman (1988). Most Drugs That Reverse Multidrug Resistance Also Inhibit Photoaffinity-Labeling of P-Glycoprotein by a Vinblastine Analog. *Mol. Pharmacol.*, Vol.33, No.2, pp.144-147, ISSN 0026-895X.

Cai, J. & P. C. H. Li (2007). Chemical Separation of Bioactive Licorice Compounds Using Capillary Electrophoresis. *J Liq. Chromatogr. Related Technol.* , Vol.30, 2805-2817, ISSN 1082-6076.

Chen, C. & A. Folch (2006). A high-performance elastomeric patch clamp chip. *Lab Chip*, Vol.6, No.10, pp.1338-45, ISSN 1473-0197 (Print).

Cheng, W., N. Klauke, H. Sedgwick, G. L. Smith & J. M. Cooper (2006). Metabolic monitoring of the electrically stimulated single heart cell within a microfluidic platform. *Lab Chip*, Vol.6, No.11, pp.1424-31, ISSN 1473-0197 (Print).

Dai, L. & Y. Chen (1999). Recent major advances in the studies on qinghaosu and related antimalarial agents. *Chemtracts*, Vol.12, 687-694, ISSN 1431-9268.

Davey, M. W., R. M. Hargrave & R. A. Davey (1996). Comparison of drug accumulation in P-glycoprotein-expressing and MRP-expressing human leukaemia cells. *Leuk. Res.*, Vol.20, No.8, pp.657-64, ISSN 0145-2126 (Print) 0145-2126 (Linking).

Dean, M. (2009). ABC transporters, drug resistance, and cancer stem cells. *JMammary Gland Biol Neoplasia*, Vol.14, No.1, pp.3-9, ISSN 1573-7039 (Electronic)1083-3021 (Linking).

Dean, M., T. Fojo & S. Bates (2005). Tumour stem cells and drug resistance. *Nat Rev Cancer*, Vol.5, No.4, pp.275-84, ISSN 1474-175X (Print).

Di Carlo, D., N. Aghdam & L. P. Lee (2006). Single-cell enzyme concentrations, kinetics, and inhibition analysis using high-density hydrodynamic cell isolation arrays. *Anal. Chem.*, Vol.78, No.14, pp.4925-30, ISSN 0003-2700 (Print).

Di Carlo, D. & L. P. Lee (2006). Dynamic single-cell analysis for quantitative biology. *Anal. Chem.*, Vol.78, No.23, pp.7918-25, ISSN 0003-2700 (Print).

Donnenberg, V. S. & A. D. Donnenberg (2005). Multiple drug resistance in cancer revisited: the cancer stem cell hypothesis. *JClin Pharmacol*, Vol.45, No.8, pp.872-7, ISSN 0091-2700 (Print) 0091-2700 (Linking).

Efferth, T., M. Davey, A. Olbrich, G. Rucker, E. Gebhart & R. Davey (2002). Activity of drugs from traditional Chinese medicine toward sensitive and MDR1- or MRP1-overexpressing multidrug-resistant human CCRF-CEM leukemia cells. *Blood Cells Mol. Dis.*, Vol.28, No.2, pp.160-8, ISSN 1079-9796 (Print).

El-Ali, J., P. K. Sorger & K. F. Jensen (2006). Cells on chips. *Nature*, Vol.442, No.7101, pp.403-11, ISSN 1476-4687 (Electronic) 0028-0836 (Linking).

Faley, S., K. Seale, J. Hughey, D. K. Schaffer, S. VanCompernolle, B. McKinney, F. Baudenbacher, D. Unutmaz & J. P. Wikswo (2008). Microfluidic platform for real-time signaling analysis of multiple single T cells in parallel. *Lab on a Chip*, Vol.8, No.10, pp.1700-12, ISSN 1473-0197 (Print) 1473-0189 (Linking).

Fallica, B., G. Makin & M. H. Zaman (2011). Bioengineering approaches to study multidrug resistance in tumor cells. *Integr Biol (Camb)*, ISSN 1757-9708 (Electronic) 1757-9694 (Linking).

Fu, D. & B. D. Roufogalis (2007). Actin disruption inhibits endosomal traffic of P-glycoprotein-EGFP and resistance to daunorubicin accumulation. *Am. J Physiol. Cell Physiol.*, Vol.292, No.4, pp.C1543-52, ISSN 0363-6143 (Print).

Gillet, J. P., T. Efferth & J. Remacle (2007). Chemotherapy-induced resistance by ATP-binding cassette transporter genes. *Biochim. Biophys. Acta*, Vol.1775, No.2, pp.237-62, ISSN 0006-3002 (Print).

Gros, P., Y. B. Ben Neriah, J. M. Croop & D. E. Housman (1986). Isolation and expression of a complementary DNA that confers multidrug resistance. *Nature*, Vol.323, No.6090, pp.728-31, ISSN 0028-0836 (Print).

Higgins, C. F. (2007). Multiple molecular mechanisms for multidrug resistance transporters. *Nature*, Vol.446, No.7137, pp.749-57, ISSN 1476-4687 (Electronic).

Hong, J. W., V. Studer, G. Hang, W. F. Anderson & S. R. Quake (2004). A nanoliter-scale nucleic acid processor with parallel architecture. *Nat. Biotechnol.*, Vol.22, No.4, pp.435-9, ISSN 1087-0156 (Print)1087-0156 (Linking).

Hsu, Y. L., P. L. Kuo & C. C. Lin (2005). Isoliquiritigenin induces apoptosis and cell cycle arrest through p53-dependent pathway in Hep G2 cells. *Life Sci*, Vol.77, No.3, pp.279-92, ISSN 0024-3205 (Print).

Hu, X. F., M. de Luise, T. J. Martin & J. R. Zalcberg (1990). Effect of cyclosporin and verapamil on the cellular kinetics of daunorubicin. *Eur. J Cancer*, Vol.26, No.7, pp.814-7, ISSN 0959-8049 (Print) 0959-8049 (Linking).

Jeffries, G. D., J. S. Edgar, Y. Zhao, J. P. Shelby, C. Fong & D. T. Chiu (2007). Using polarization-shaped optical vortex traps for single-cell nanosurgery. *Nano Lett*, Vol.7, No.2, pp.415-20, ISSN 1530-6984 (Print)1530-6984 (Linking).

Jow, G. M., C. J. Chou, B. F. Chen & J. H. Tsai (2004). Beauvericin induces cytotoxic effects in human acute lymphoblastic leukemia cells through cytochrome c release, caspase 3 activation: the causative role of calcium. *Cancer Lett.*, Vol.216, No.2, pp.165-73, ISSN 0304-3835 (Print).

Kanazawa, M., Y. Satomi, Y. Mizutani, O. Ukimura, A. Kawauchi, T. Sakai, M. Baba, T. Okuyama, H. Nishino & T. Miki (2003). Isoliquiritigenin inhibits the growth of prostate cancer. *Eur Urol*, Vol.43, No.5, pp.580-6, ISSN 0302-2838 (Print).

Klauke, N., G. L. Smith & J. Cooper (2003). Stimulation of single isolated adult ventricular myocytes within a low volume using a planar microelectrode array. *Biophys. J*, Vol.85, No.3, pp.1766-74, ISSN 0006-3495 (Print).

Li, P. C. H., L. de Camprieu, J. Cai & M. Sangar (2004). Transport, retention and fluorescent measurement of single biological cells studied in microfluidic chips. *Lab Chip*, Vol.4, No.3, pp.174-180, ISSN 1473-0189.

Li, X., Y. Chen & P. C. Li (2011). A simple and fast microfluidic approach of same-single-cell analysis (SASCA) for the study of multidrug resistance modulation in cancer cells. *Lab Chip*, Vol.11, No.7, pp.1378-84, ISSN 1473-0189 (Electronic) 1473-0189 (Linking).

Li, X. J., J. Huang, G. F. Tibbits & P. C. H. Li (2007). Real-time monitoring of intracellular calcium dynamic mobilization of a single cardiomyocyte in a microfluidic chip pertaining to drug discovery. *Electrophoresis*, Vol.28, No.24, pp.4723-4733, ISSN 0173-0835.

Li, X. J. & P. C. H. Li (2005). Microfluidic selection and retention of a single cardiac myocyte, on-chip dye loading, cell contraction by chemical stimulation, and quantitative fluorescent analysis of intracellular calcium. *Anal. Chem.*, Vol.77, No.14, pp.4315-4322, ISSN 0003-2700.

Li, X. J. & P. C. H. Li (2006). Contraction study of a single cardiac muscle cell in a microfluidic chip. *Methods Mol. Biol.*, Vol.321, 199-225, ISSN 1064-3745 (Print).

Li, X. J. & P. C. H. Li (2010). Strategies for the real-time detection of Ca2+ channel events of single cells: recent advances and new possibilities. *Expert Rev. Clin. Pharmacol.*, Vol.3, 267-280, ISSN 1751-243.

Li, X. J., V. Ling & P. C. H. Li (2008). Same-single-cell analysis for the study of drug efflux modulation of multidrug resistant cells using a microfluidic chip. *Anal. Chem.*, Vol.80, No.11, pp.4095-4102, ISSN 0003-2700.

Li, X. J., X. Xue & P. C. H. Li (2009). Real-time detection of the early event of cytotoxicity of herbal ingredients on single leukemia cells studied in a microfluidic biochip. *Integr. Biol.*, Vol.1, No.1, pp.90-98, ISSN 1757-9694.

Liu, P., X. Li, S. A. Greenspoon, J. R. Scherer & R. A. Mathies (2011). Integrated DNA purification, PCR, sample cleanup, and capillary electrophoresis microchip for forensic human identification. *Lab Chip*, Vol.11, No.6, pp.1041-8, ISSN 1473-0189 (Electronic)1473-0189 (Linking).

Locke, V. L., R. A. Davey & M. W. Davey (2003). Modulation of drug and radiation resistance in small cell lung cancer cells by paclitaxel. *Anticancer Drugs*, Vol.14, No.7, pp.523-31, ISSN 0959-4973 (Print).

Ma, J., N. Y. Fu, D. B. Pang, W. Y. Wu & A. L. Xu (2001). Apoptosis induced by isoliquiritigenin in human gastric cancer MGC-803 cells. *Planta Med*, Vol.67, No.8, pp.754-7, ISSN 0032-0943 (Print).

Manz, A., D. J. Harrison, E. M. J. Verpoorte, J. C. Fettinger, A. Paulus, H. Ludi & H. M. Widmer (1992). Planar Chips Technology for Miniaturization and Integration of Separation Techniques into Monitoring Systems - Capillary Electrophoresis on a Chip. *J Chromatogr.*, Vol.593, No.1-2, pp.253-258, ISSN 0021-9673.

Marthinet, E., G. Divita, J. Bernaud, D. Rigal & L. G. Baggetto (2000). Modulation of the typical multidrug resistance phenotype by targeting the MED-1 region of human MDR1 promoter. *Gene. Ther.*, Vol.7, No.14, pp.1224-33, ISSN 0969-7128 (Print).

Meaden, E. R., P. G. Hoggard, S. H. Khoo & D. J. Back (2002). Determination of P-gp and MRP1 expression and function in peripheral blood mononuclear cells in vivo. *J Immunol. Methods*, Vol.262, No.1-2, pp.159-65, ISSN 0022-1759 (Print).

Medeiros, B. C., H. J. Landau, M. Morrow, R. O. Lockerbie, T. Pitts & S. G. Eckhardt (2007). The farnesyl transferase inhibitor, tipifarnib, is a potent inhibitor of the MDR1 gene product, P-glycoprotein, and demonstrates significant cytotoxic synergism against human leukemia cell lines. *Leukemia*, Vol.21, No.4, pp.739-46, ISSN 0887-6924 (Print).

Murthy, R. S. R. & N. M. Shah (2007). Strategies for inhibition of P-glycoproteins for effective treatment of multidrug resistance tumors. *J Biomed. Nanotechnol.*, Vol.3, No.1, pp.1-17, ISSN 1550-7033.

Peng, X. Y. & P. C. Li (2005). Extraction of pure cellular fluorescence by cell scanning in a single-cell microchip. *Lab Chip*, Vol.5, No.11, pp.1298-302, ISSN 1473-0197 (Print).

Peng, X. Y. & P. C. H. Li (2004). A three-dimensional flow control concept for single-cell experiments on a microchip. 1. Cell selection, cell retention, cell culture, cell balancing, and cell scanning. *Anal. Chem.*, Vol.76, No.18, pp.5273-5281, ISSN 0003-2700.

Peng, X. Y. & P. C. H. Li (2004). A three-dimensional flow control concept for single-cell experiments on a microchip. 2. Fluorescein diacetate metabolism and calcium mobilization in a single yeast cell as stimulated by glucose and pH changes. *Anal. Chem.*, Vol.76, No.18, pp.5282-92, ISSN 0003-2700 (Print).

Perez-Tomas, R. (2006). Multidrug resistance: retrospect and prospects in anti-cancer drug treatment. *Curr. Med. Chem.*, Vol.13, No.16, pp.1859-76, ISSN 0929-8673 (Print).

Persidis, A. (1999). Cancer multidrug resistance. *Nat. Biotechnol.*, Vol.17, No.1, pp.94-5, ISSN 1087-0156 (Print).

Ren, Y. & D. Wei (2004). Quantification intracellular levels of oligodeoxynucleotide-doxorubicin conjugate in human carcinoma cells in situ. *J. Pharm. Biomed. Anal.*, Vol.36, No.2, pp.387-91, ISSN 0731-7085 (Print).

Ryttsen, F., C. Farre, C. Brennan, S. G. Weber, K. Nolkrantz, K. Jardemark, D. T. Chiu & O. Orwar (2000). Characterization of single-cell electroporation by using patch-clamp and fluorescence microscopy. *Biophys J*, Vol.79, No.4, pp.1993-2001, ISSN 0006-3495 (Print) 0006-3495 (Linking).

Salieb-Beugelaar, G. B., G. Simone, A. Arora, A. Philippi & A. Manz (2010). Latest developments in microfluidic cell biology and analysis systems. *Anal. Chem.*, Vol.82, No.12, pp.4848-64, ISSN 1520-6882 (Electronic) 0003-2700 (Linking).

Schumann, C. A., A. Dorrenhaus, J. Franzke, P. Lampen, P. S. Dittrich, A. Manz & P. H. Roos (2008). Concomitant detection of CYP1A1 enzymatic activity and CYP1A1 protein in individual cells of a human urothelial cell line using a bilayer microfluidic device. *Anal. Bioanal. Chem.*, Vol.392, No.6, pp.1159-66, ISSN 1618-2650 (Electronic).

Shervington, A. & C. Lu (2008). Expression of multidrug resistance genes in normal and cancer stem cells. *Cancer Invest*, Vol.26, No.5, pp.535-42, ISSN 1532-4192 (Electronic) 0735-7907 (Linking).

Sims, C. E. & N. L. Allbritton (2007). Analysis of single mammalian cells on-chip. *Lab Chip*, Vol.7, No.4, pp.423-40, ISSN 1473-0197 (Print).

Sung, M. W. & P. C. Li (2004). Chemical analysis of raw, dry-roasted, and honey-roasted licorice by capillary electrophoresis. *Electrophoresis*, Vol.25, No.20, pp.3434-40, ISSN 0173-0835 (Print) 0173-0835 (Linking).

Thomas, H. & H. M. Coley (2003). Overcoming multidrug resistance in cancer: an update on the clinical strategy of inhibiting p-glycoprotein. *Cancer Control*, Vol.10, No.2, pp.159-65, ISSN 1073-2748 (Print).

Wang, E. J., C. N. Casciano, R. P. Clement & W. W. Johnson (2000). In vitro flow cytometry method to quantitatively assess inhibitors of P-glycoprotein. *Drug Metab. Dispos.*, Vol.28, No.5, pp.522-8, ISSN 0090-9556 (Print).

Wang, M. M., E. Tu, D. E. Raymond, J. M. Yang, H. Zhang, N. Hagen, B. Dees, E. M. Mercer, A. H. Forster, I. Kariv, P. J. Marchand & W. F. Butler (2005). Microfluidic sorting of mammalian cells by optical force switching. *Nat. Biotechnol.*, Vol.23, No.1, pp.83-7, ISSN 1087-0156 (Print).

Wang, Q., L. Wu, Y. Zhao, X. L. Zhang & N. wang (2002). The anticancer effect of artesunate and its mechanism. *Acta Pharmaceutica Sinica*, Vol.37, 477-478, ISSN 0513-4870.

Warmann, S., G. Gohring, B. Teichmann, H. Geerlings & J. Fuchs (2002). MDR1 modulators improve the chemotherapy response of human hepatoblastoma to doxorubicin in vitro. *J Pediatr. Surg.*, Vol.37, No.11, pp.1579-84, ISSN 1531-5037 (Electronic) 0022-3468 (Linking).

Wheeler, A. R., W. R. Throndset, R. J. Whelan, A. M. Leach, R. N. Zare, Y. H. Liao, K. Farrell, I. D. Manger & A. Daridon (2003). Microfluidic device for single-cell analysis. *Anal. Chem.*, Vol.75, No.14, pp.3581-6, ISSN 0003-2700 (Print).

Zeng, Y., R. Novak, J. Shuga, M. T. Smith & R. A. Mathies (2010). High-performance single cell genetic analysis using microfluidic emulsion generator arrays. *Anal. Chem.*, Vol.82, No.8, pp.3183-90, ISSN 1520-6882 (Electronic) 0003-2700 (Linking).

Cancer Stem Cells - The Cutting Edge

Edited by Prof. Stanley Shostak

ISBN 978-953-307-580-8
Hard cover, 606 pages
Publisher InTech
Published online 01, August, 2011
Published in print edition August, 2011

Over the last thirty years, the foremost inspiration for research on metastasis, cancer recurrence, and increased resistance to chemo- and radiotherapy has been the notion of cancer stem cells.The twenty-eight chapters assembled in Cancer Stem Cells - The Cutting Edge summarize the work of cancer researchers and oncologists at leading universities and hospitals around the world on every aspect of cancer stem cells, from theory and models to specific applications (glioma), from laboratory research on signal pathways to clinical trials of bio-therapies using a host of devices, from solutions to laboratory problems to speculation on cancersâ€™ stem cellsâ€™ evolution. Cancer stem cells may or may not be a subset of slowly dividing cancer cells that both disseminate cancers and defy oncotoxic drugs and radiation directed at rapidly dividing bulk cancer cells, but research on cancer stem cells has paid dividends for cancer prevention, detection, targeted treatment, and improved prognosis.

How to reference

In order to correctly reference this scholarly work, feel free to copy and paste the following:

XiuJun Li, Yuchun Chen and Paul C.H. Li (2011). Modulation of Multidrug Resistance on the Same Single Cancer Cell in a Microfluidic Chip: Intended for Cancer Stem Cell Research, Cancer Stem Cells - The Cutting Edge, Prof. Stanley Shostak (Ed.), ISBN: 978-953-307-580-8, InTech, Available from: http://www.intechopen.com/books/cancer-stem-cells-the-cutting-edge/modulation-of-multidrug-resistance-on-the-same-single-cancer-cell-in-a-microfluidic-chip-intended-fo

INTECH
open science | open minds

InTech Europe
University Campus STeP Ri
Slavka Krautzeka 83/A
51000 Rijeka, Croatia
Phone: +385 (51) 770 447
Fax: +385 (51) 686 166
www.intechopen.com

InTech China
Unit 405, Office Block, Hotel Equatorial Shanghai
No.65, Yan An Road (West), Shanghai, 200040, China
中国上海市延安西路65号上海国际贵都大饭店办公楼405单元
Phone: +86-21-62489820
Fax: +86-21-62489821

IntechOpen